Enhanced Fluorescence Resonance Energy Transfer between Spectral Variants of Green Fluorescent Protein through Zinc-Site Engineering

Kristian K. Jensen, Lene Martini, and Thue W. Schwartz*

Laboratory for Molecular Pharmacology, Department of Pharmacology, The Panum Institute, University of Copenhagen, Copenhagen, Denmark

Received July 27, 2000; Revised Manuscript Received November 2, 2000

ABSTRACT: Although spectral variants of GFP should in theory be suited for fluorescence resonance energy transfer (FRET) and therefore suited for studies of protein−protein interactions, the unfavorable location of the fluorophore 15 Å deep inside the GFP molecule has especially impaired this application. Here, metal-ion site engineering around the dimerization interface known from the X-ray structure of GFP is applied to the cyan and the yellow spectral variant of GFP to stabilize the heterodimeric form of these molecules and thereby increase FRET signaling. The FRET signal, determined as the ratio between the maximal emission for the yellow variant, 530 nm, and the cyan variant, 475 nm, during excitation of the cyan variant at 433 nm was increased up to 8−10-fold in the presence of 10^{-4} M $ZnCl_2$ by engineering of two symmetric metal-ion sites being either bidentate or tridentate. A similar increase in FRET signaling was however obtained in a pair of molecules in which a single bidentate metal-ion site was generated by introducing a zinc-binding residue in each of the two spectral variants of GFP and therefore creating an obligate heterodimeric pair. It is concluded that FRET signaling between spectral variants of GFP can be increased by stabilizing dimer formation and especially by favoring heterodimer formation in this case performed by metal-ion site engineering.

Green fluorescent protein (GFP)[1] is one of the most widely used tools in cell biology, for example, for studying gene expression or protein localization and trafficking within cells (*1*). It is a very versatile genetic tag as it can be fused to the protein of interest and the resulting chimeric protein can be studied in living cells, for example, after transfection or even in transgenic animals. The development of color variants of GFP having distinct spectral properties has made it possible to exploit fluorescence resonance energy transfer (FRET) between such spectral variants in cellular studies (*2*). FRET is a nonradiative exchange of energy between two fluorescent molecules, one functioning as a donor of energy to an acceptor, which is excited and emits at a longer wavelength (*3*). In theory GFP-based FRET is an attractive method for studies of protein−protein interactions within living cells (*4*). For example, genetic tagging of proteins with GFP usually renders fully functional chimeric proteins, that may be expressed and targeted normally to specific organelles within the cell (*4*). Nevertheless, despite the fact that the physical characteristics of FRET have been known for many years and that both the GFP variants and the instrumentation for the detection of FRET are readily available, surprisingly few publications documenting protein−protein interactions by use of GFP-based FRET have been published (*5*−*10*). The problem is that although GFP and its spectral variants from a protein chemistry and molecular biology point-of-view in many ways are ideal fluorescent tags, they have some biophysical shortcomings. First, the potential FRET donors, BFP (blue), for GFP, and CFP (cyan), for YFP (yellow), fluoresce with relatively low intensity. Second, the emission spectra of the donor and acceptor pairs are not fully separated, which may give rise to false FRET signals. Importantly, in FRET, the energy transfer is highly dependent on the distance between the donor and the acceptor molecules (*3*). According to Förster, the efficiency of FRET is given by the expression $R_0^6/(R_0^6 + r^6)$, where r is the actual distance separating the fluorophores of the donor and acceptor molecules, and R_0 is the distance at which the efficiency of FRET is 50% (*3*). R_0 is determined by spectral characteristics of the donor and acceptor fluorophores and by the relative orientation of the fluorophores. The R_0 values of the GFP variants used in FRET studies are in the range 40−50 Å, assuming random orientation of the fluorophores (*4*). However, a 100% efficiency of FRET is not possible to achieve between color variants of GFP, since the fluorophore is buried approximately 15 Å from the surface of the GFP molecule, causing the lowest possible distance between the two fluorophores to be about 30 Å (*11*, *12*). Also, because the efficiency of FRET depends on the inverse sixth power of the distance, the absolute limit for successful detection of FRET is $2 \times R_0$ (*13*). Thus, although two proteins of interest genetically tagged with color variants of GFP do in fact interact, the FRET signal may be too weak for effective detection due to inadequate proximity of the two fluorescent

* To whom correspondence should be addressed. Thue W. Schwartz, Laboratory for Molecular Pharmacology, Department of Pharmacology, The Panum Institute, Blegdamsvej 3C, DK-2200, Copenhagen, Denmark. E-mail: schwartz@molpharm.dk. Phone: +45 3532 7603. Fax: +45 3535 2995.

[1] Abbreviations: GFP: green fluorescent protein; BFP: blue fluorescent protein; CFP: cyan fluorescent protein; YFP: yellow fluorescent protein; FP: fluorescent protein; FRET: fluorescence resonance energy transfer.

10.1021/bi001765m CCC: $20.00
Published on Web 01/03/2001

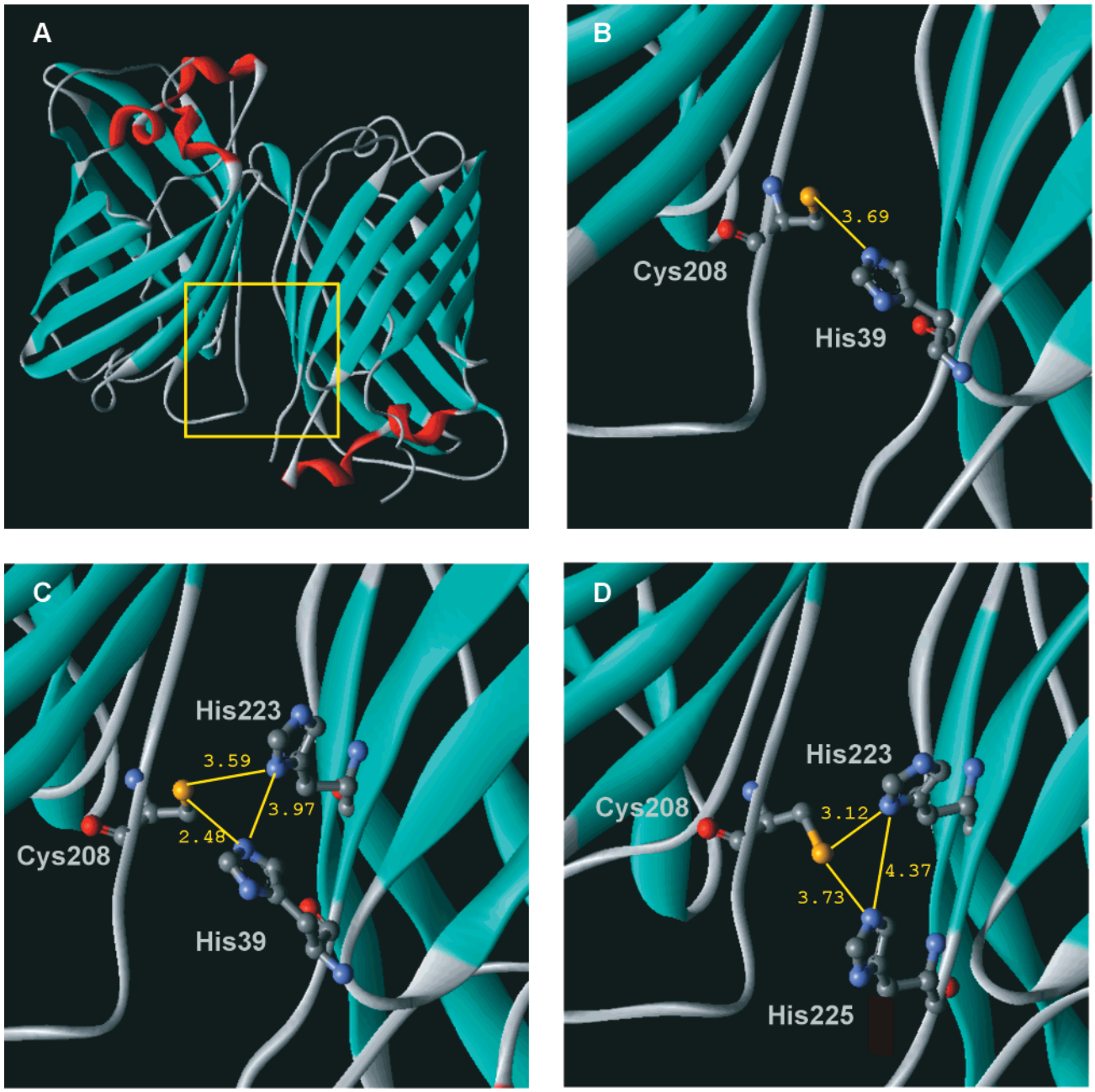

FIGURE 1: GFP dimer with engineered zinc sites. The Zn(II)-binding sites were constructed on the basis of the structure of the GFP dimer of Yang et al. (PDB entry code 1GFL). Panel A: the crystal structure of the GFP homodimer. Panel B: the putative Zn(II)-binding site composed of the [S208C] mutation facing the [Y39H] mutation. This motif is thought to give rise to one bidentate zinc site in the [S208C]-CFP/[Y39H]-YFP pair and two bidentate sites in the [Y39H,S208C]-CFP/[Y39H,S208C]-YFP pair. Panel C: the [S208C] mutation facing the [Y39H,F223H] double mutation. This motif is thought to give rise to two tridentate sites in the [Y39H,S208C,F223H]-CFP/[Y39H,-S208C,F223H]-YFP pair. Panel D: the [S208C] mutation facing the [F223H,T225H] double mutation. This motif is also presumed to give rise to two tridentate sites.

probes and/or nonoptimal orientation of the fluorophores (*4*). This may especially be the case if detection of the interactions is based on fluorescence microscopy of cells, a method that suffers from relatively high background fluorescence (*4*).

The X-ray structure of GFP has demonstrated that the protein folds into a highly characteristic 11-stranded β-barrel structure which is efficiently closed off at both ends and accordingly the structure is called a β-can (*11*, *12*). The crystal structure of GFP as well as studies of GFP variants in solution have revealed the tendency of this protein to form 2-fold symmetric dimers (Figure 1, panel A) (*11*). In the dimeric form of GFP, the fluorophores of the two monomers are brought into the closest possible proximity and in an orientation which is suitable for exchange of energy through FRET. Thus, the formation of a dimer between CFP and YFP should be optimal with regard to FRET (*4*). Unfortunately, dimer formation of GFP requires relatively high concentrations of the protein (*14*). In the present study, we have used the crystal structure of the wild-type GFP dimers as a template for the introduction of stabilizing zinc-binding sites in the interface between the two monomers, and we show that the FRET signal derived from the zinc-sites engineered cyan and yellow variants of GFP can be increased 8−10-fold in the presence of divalent zinc ions.

MATERIALS AND METHODS

Construction of Zinc-Site Modified CFP and YFP. All constructs were based on the GFP variants ECFP and EYFP from Clontech (Palo Alto, CA). The point mutations were introduced in the CFP and YFP cDNA by the polymerase chain reaction overlap extension technique (*15*). All reactions were carried out using the *pfu* polymerase (Stratagene, La Jolla, CA) under conditions recommended by the manufacturer. The generated mutated cDNA was cloned into the pUC19-derived pECFP vector by substituting the original CFP cDNA with the mutated CFP or YFP cDNA. The mutations were verified by restriction endonuclease digestion and DNA sequencing using the Thermo Sequenase fluorescent-labeled primer cycle sequencing kit with 7-deaza-dGTP on an Alfexpress DNA sequencer according to the manufacturer's instructions (Amersham Pharmacia Biotech, Uppsala, Sweden). Accordingly, the four CFP constructs: [Y39H]; [Y39H,S208C]; [Y39H,S208C,F223H]; and [S208C,F223H,T225H] and the four YFP constructs: [S208C]; [Y39H,S208C]; [Y39H,S208C,F223H]; and [S208C,F223H,T225C], were generated.

Construction of Covalently Linked CFP and YFP. Two DNA primers encoded a linker, with the amino acid sequence GANSPSANIEGRNASPSNAG, containing the Factor Xa cleavage site, IEGR. The antisense primer (5′-GGCATGGACGAGCTGTACAAGGGAGCGAATTCACCATC-3′), containing a 3′ *Eco*RI site, was used to clone CFP from the pECFP vector. The sense primer (5′-CGGAGCGAATTCACCATCCGCAAATATAGAAGGC-CGAAACGCCAGTCCCAGCAATGCCGG-GATGGTGAGCAAGGGCGAGGAGG-3′), containing a 5′ *Eco*RI site, was used to clone YFP from the pEYFP vector. The CFP PCR fragment was cut with *Nco*I and *Eco*RI, the YFP PCR fragment was cut with *Eco*RI and *Not*I, and the two fragments were cloned into the pECFP vector from which the CFP cDNA had been excised with *Nco*I and *Not*I. *Pfu* polymerase (Stratagene) was used in the PCR reactions. The final construct was verified by restriction endonuclease digestion and DNA sequencing.

Expressing of Wild Type, Mutated CFP and YFP, and Covalently Linked CFP and YFP in Escherichia coli. Competent *E. coli* BL21- (DE3) cells were transformed with the pECFP vector containing the construct of interest and cultured overnight in 20 mL of LB medium supplemented with 250 μg/mL ampicillin. The overnight culture was diluted 100-fold into 0.5 L of medium and shaken at 37 °C until $A_{550} = 0.4-0.6$. Protein expression was then initiated by adding isopropyl-beta-D-thiogalactopyranoside (IPTG) to a final concentration of 1.0 mM and shaken for another 4 h. The cells were harvested by centrifugation and resuspended in 30 mL of lysis buffer (50 mM Tris-Cl, pH 8.0, 100 mM NaCl, 0.33 mg/mL lysozyme, 0.5 mg/mL DNase), incubated for 1 h at room temperature (30 min for the covalently linked CFP and YFP), diluted to 90 mL with H_2O and finally frozen and thawed. Cell debris were removed by centrifugation (17000*g*, 15 min). The supernatant was applied to at column containing 10 mL of phenyl-sepharose CL-4B gel (Amersham Pharmacia Biotech) preequilibrated with 30 mL of 25 mM NaCl. The column was washed using 15 mL of 25 mM NaCl, and protein was eluted in fractions of 1 mL using H_2O. The concentration of either CFP or YFP in the eluted fractions was determined by measuring the absorption at 433 or 523 nm, respectively.

Fluorescence Spectroscopy. Fluorescence spectroscopy was performed at room temperature on a SPEX Fluoromax spectrofluorometer with photon counting mode using an excitation and emission band-pass of 4.2 nm. Measurements were done on 1-mL cylindrical glass cuvettes containing 300 μL continuously stirred fluorescent protein solution.

CFP-linker-YFP cleavage was performed in a buffer containing 100 mM NaCl, 2.0 mM $CaCl_2$, and 20 mM Tris-Cl (pH 8.0) and approximately 0.1 μM of the CFP-linker-YFP construct. Factor Xa, 10 μL of 1.0 μg/μL, was added, and the emission spectra were recorded at various time points. Slit widths were 2.5 nm, and the increment was 2 s/nm. The Zn(II) studies were performed on solutions containing 10 μM of both of the two fluorescent proteins in 20 mM Tris-Cl adjusted to pH 8.0. Fifteen microliters of 20× $ZnCl_2$ stocks were added starting at 10^{-5} M and increasing the concentration in the same probe in steps to a final concentration of 10^{-2} M $ZnCl_2$. The slit width was 1.2 nm, and the increment was 0.25 s/nm.

RESULTS

Design of the Zn-Binding Sites. Because of the favorable spectral properties, we chose to build the metal-ion sites into the interface of dimers of CFP and YFP. In the X-ray structure of GFP, we searched for residues in the dimer interface that would be located in an appropriate distance to form a metal-ion binding site when substituted with either His or Cys residues and that would be readily accessible from the solvent. For a bivalent site, we chose Tyr^{39} and Ser^{208} located on each of the monomers of CFP and YFP (Figure 1, panel B). When substituted to His and Cys, respectively, the electron donating atoms would be approximately 4 Å apart, a distance that should be optimal for the coordination of Zn(II), i.e., assuming that the side chains would adopt a similar conformation as the native Tyr^{39} and Ser^{208} residues (*16*). Moreover, the substitutions, [Y39H, S208C], would be expected to cause rather little steric disturbance in the dimerization interface due to the relatively similar size of the native and the introduced residues. Finally, residues 39 and 208 should be readily accessible for Zn(II) from the aqueous phase.

In the attempt to construct a tridentate metal-ion site, two additional residues in the vicinity of residues 39 and 208 were addressed, Phe^{223} and Thr^{225}, which both are located on the most C-terminal β-strand of the barrel. As shown in Figure 1, panel C, substitution of Phe^{223} with a His in a monomer with the [Y39H] substitution would, when dimerized with another GFP molecule expressing the [S208C] substitution, bring three metal-ion coordinating residues in close enough proximity to conceivably be able to form a tridentate metal-ion binding site. Similarly, two His residues introduced at "neighboring" positions on the exterior face of the last β-sheet in the GFP structure, i.e., at positions 223 and 225, should when combined with a [S208C]-GFP molecule also be able to form a suitable metal-ion binding site (Figure 1, panel D).

On the basis of these predictions, four types of Zn(II)-site modified FRET pairs were constructed: (i) CFP and YFP both containing the [Y39H] and [S208C] mutations (Figure

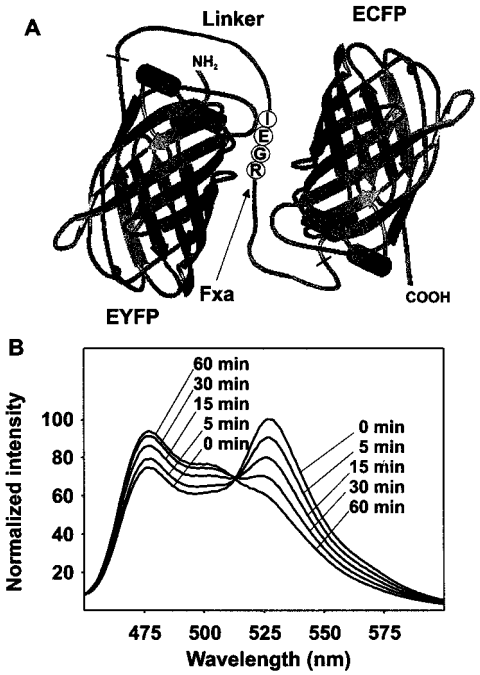

FIGURE 2: Spectrofluorometric analysis of covalently linked CFP and YFP. Panel A: schematic drawing of the covalently linked CFP and YFP construct. The linker sequence is GANSPSANI-EGRNASPSNAG, containing a centrally placed Factor Xa cleavage site, IEGR. Panel B: emission spectra taken at various time points during enzymatic digest of the CFP−YFP fusion protein and excited at 433 nm, the excitation maximum for CFP.

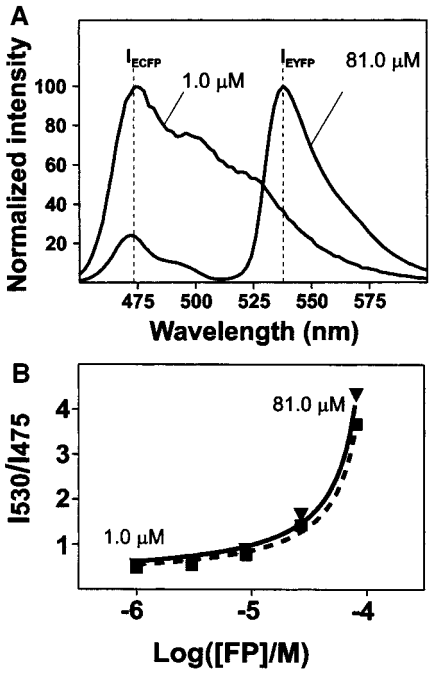

FIGURE 3: Relationship between concentration of fluorescent proteins and FRET signal. Panel A: normalized emission spectra of equimolar mixtures of CFP and YFP at concentrations of 1.0 and 81 μM, excited at 433 nm. Panel B: the ratio between the YFP (acceptor) emission peak, I_{530}, and the CFP (donor) emission peak, I_{475} (i.e., the "FRET signal"), shown as a function of the concentration of the wild-type CFP/YFP (■) and the [S208C,-F223H,T225H]-CFP/[S208C,F223H,T225C]-YFP (▼) donor−acceptor mixtures. The increasing FRET signal is presumably a result of the intrinsic tendency of GFP variants to form dimers in solution.

1, panel B). Because of the symmetry of the dimer, these substitutions should be able to form two bidentate sites. (ii) CFP and YFP both containing the [Y39H], [S208C], and [F223H] mutations, presumably giving rise to two tridentate sites (Figure 1, panel C). (iii) CFP with the mutations [S208C], [F223H], and [T225H] and YFP with the mutations [S208C], [F223H], and [T225C] (Figure 1, panel D), which also should be able to form two tridentate sites. YFP with a [T225H] substitution could, for unknown reasons, not be expressed in *E. coli*. (iv) CFP containing the [S208C] mutation and YFP containing the [Y39H] mutation. The latter pair should in theory upon metal-ion binding preferentially combine in heterodimers of CFP and YFP and not be able to form, with respect to FRET, the nonproductive homodimers between each of the spectral variants.

FRET between Covalently Linked CFP and YFP. As a positive FRET control, we made a construct in which CFP and YFP were linked by a 20-amino acid linker containing a Factor Xa cleavage site (residues IEGR) (Figure 2, panel A). This construct was expressed in *E. coli* and studied by spectrofluometry. When excited at 433 nm, i.e., the excitation wavelength for CFP, this construct had an emission spectrum with a minor peak corresponding to the emission maximum for CFP, 475 nm, but the spectrum was dominated by an even higher maximum at 530 nm, i.e., the emission maximum for YFP (Figure 2, panel B). This indicates that efficient energy transfer occurs from CFP to YFP in the covalently linked construct. When this construct was exposed to the enzyme Factor Xa, the YFP emission gradually decreased and the CFP emission gradually increased as the binary fluorescent protein construct conceivably was degraded to monomeric CFP and YFP (Figure 2, panel B). In the following, the FRET signal is arbitrarily expressed as the ratio between the fluorescence intensity measured at 530 nM and at 475 nM, i.e., I_{530}/I_{475}.

Concentration Dependency of FRET between CFP and YFP. The dissociation constant for dimerization of wild-type GFP has been estimated to be 100 μM (*14*). To distinguish autodimerization and zinc-induced dimerization, the concentration dependency of the FRET signal between "wild type" CFP and YFP was studied. As shown in Figure 3, in a solution with a mixture of 1 μM of each of the spectral variants of GFP, excitation with 433 nm gave an almost pure CFP spectrum. By increasing the concentrations of the proteins, an increasing FRET signal (i.e., the I_{530}/I_{475} ratio) was observed. At the highest concentration tested, 81 μM, the spectrum was dominated by the YFP component (Figure 3, panel A, note the relative scale).

The spectral properties, i.e., the emission and excitation spectra, of the mutated CFP and YFP molecules were determined and showed no divergence from the wild-type spectra (data not shown). As shown in Figure 3, panel B, the concentration-dependent increase in the FRET signal was very similar even for the triple mutated proteins, i.e., the [Y39H,S208C,F223H]-CFP/[Y39H,S208C,F223H]-YFP pair, indicating that the basic dimerization property of the mutant proteins is similar to that of the wild-type proteins and of GFP (*14*). The following studies with the zinc-site engineered YFP and CFP were performed at 10 μM at which concentration only minimal autodimerization is observed as judged by the FRET signal (Figure 3, panel B).

Zinc-Induced FRET in the Bidentate Metal-Ion Site Engineered Proteins. The effect of increasing concentrations

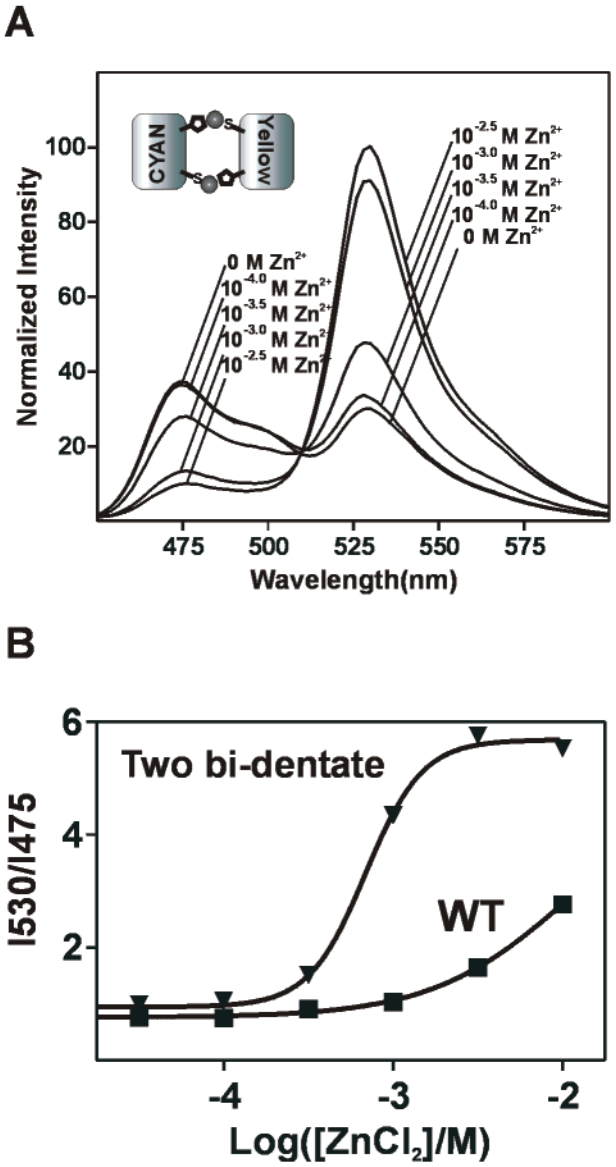

FIGURE 4: Emission spectra of a mixture of CFP and YFP with two bidentate zinc sites in response to increasing [$ZnCl_2$]. A mixture of 10 μM [Y39H,S208C]-CFP and [Y39H,S208C]-YFP was excited at 433 nm. Panel A: the emission spectra recorded at $ZnCl_2$ concentrations from 0 to 10^{-2} M (in the upper left corner a schematic drawing showing the presumed stabilization of the dimeric conformation coursed by zinc ions). Panel B: the ratio between the YFP (acceptor) emission peak, I_{530}, and the CFP (donor) emission peak, I_{475} (i.e., the "FRET signal"), shown as a function of the concentration $ZnCl_2$ for wild type (■) and the [Y39H,S208C]-CFP/[Y39H,S208C]-YFP pair (▼).

of $ZnCl_2$ on the emission spectra of a mixture of [Y39H,-S208C]-CFP and [Y39H,S208C]-YFP is shown in Figure 4. Zn(II) induced a dose-dependent increase in the FRET signal as indicated by a decrease in CFP (donor) emission and an increase in YFP (acceptor) emission. The spectral changes closely resembled the changes that were observed in the covalently linked CFP−YFP construct upon enzyme digestion with the major difference being that the changes occurred in the opposite order as FRET was induced by increasing metal-ion concentrations (Figure 2, panel B, and Figure 4, panel A). The EC_{50} for induction of FRET in the [Y39H,S208C]-CFP and [Y39H,S208C]-YFP mixture was 0.7 mM (Figure 4, panel B). We interpret the zinc-induced increase in FRET as stabilization of a heterodimer of the

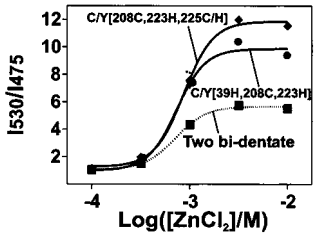

FIGURE 5: FRET signal from CFP and YFP pairs designed to be able to form tridentate metal-ion sites. The I_{530}/I_{475} ratio was determined for the two FRET pairs forming triple coordinated Zn-(II) binding sites. The experiments were made as triplicates; error bars indicate SEM. The EC50 value of the bidentate site is 0.7 mM, the EC50 value of the [S208C,F223H,T225H]-CFP/[S208C,-F223H,T225C]-YFP pair is 0.9 mM, and the EC50 value of the [Y39H,S208C,F223H]-CFP/[Y39H,S208C,F223H]-YFP pair is 0.7 mM. The [S208C,F223H,T225H]-CFP/[S208C,F223H,T225C]-YFP pair (◆), the [Y39H,S208C,F223H]-CFP/[Y39H,S208C,F223H]-YFP pair (●), and the FRET pair forming two bidentate sites [Y39H,S208C]-CFP/[Y39H], [S208C]-YFP (■).

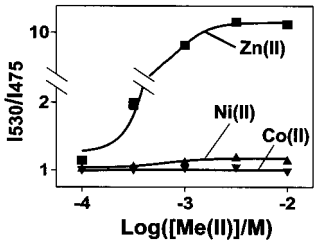

FIGURE 6: Effect of different divalent metal-ions on the FRET signal in metal-ion site engineered spectral variants of GFP. The effect of Zn(II) (■), Co(II) (▼), and Ni(II) (▲) on the [S208C,-F223H,T225H]-CFP/[S208C,F223H,T225C]-YFP pair. The experiments were made as triplicates; error bars indicate SEM.

mutated CFP and YFP molecules corresponding to the dimer found in the X-ray structure of GFP (*11*, *14*). Zn(II) also induced a FRET signal in a mixture of "wild type" CFP and YFP (Figure 4, panel B). However, this FRET signal was first detectable with high concentrations of Zn(II) (Figure 4, panel B). The zinc-induced FRET signal in the "wild-type" spectral variants of GFP might be a result of the formation of various dimers in which Zn(II) coordinates native His residues located at different locations on the surface of CFP and YFP, respectively.

Zinc-Induced FRET in the Tridentate Metal-Ion Site Engineered Proteins. The maximally achievable Zn(II)-induced FRET signal was almost 2-fold higher in the mixture of pairs of CFP and YFP with the potential to form tridentate metal-ion sites as compared to the bidentate constructs (Figure 5). The Emax was 8.9 (i.e., the maximal I_{530}/I_{475} ratio minus the baseline ratio) for the [Y39H,S208C,F223H]-CFP and [Y39H,S208C,F223H]-YFP mixture, and it was 10.6 for the [S208C,F223H,T225H]-CFP and [S208C,F223H,T225C]-YFP mixture. Surprisingly, however, the potency of Zn(II) for induction of FRET was not increased in the tridentate constructs as compared to the bidentate construct (Figure 5).

The effect of other bivalent cations in inducing FRET was tested in the most efficacious metal-ion site constructs, i.e., the mixture of [S208C,F223H,T225H]-CFP and [S208C,-F223H,T225C]-YFP. As shown in Figure 6, Co(II) had no effect, whereas Ni(II) induced a FRET signal, which however only amounted to approximately 1.3% of the maximal achievable Zn(II) response. $CaCl_2$ had no measurable effect

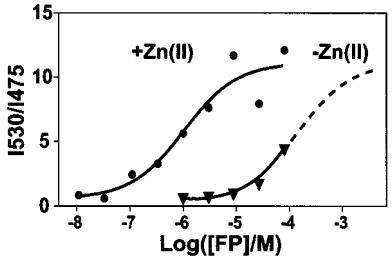

FIGURE 7: Concentration-dependent FRET signal in metal-ion site engineered spectral variants of GFP in the absence and presence of Zn(II). The ratio between the YFP (acceptor) emission peak, I_{530}, and the CFP (donor) emission peak, I_{475} (i.e., "FRET signal"), in the absence of Zn(II) (▼) or in the presence of 10^{-2} M Zn(II) (●) shown in equimolar mixtures of [S208C,F223H,T225H]-CFP and [S208C,F223H,T225C]-YFP at various concentrations.

on the FRET signal, whereas $CuSO_4$ had a destructive effect on fluorescence at all wavelengths (data not shown).

The dependency on protein concentration of the FRET signal was also determined in the absence and presence of Zn(II) in the [S208C,F223H,T225H]-CFP and [S208C,-F223H,T225C]-YFP mixture. As shown in Figure 7, in these metal-ion site engineered GFP analogues in the presence of zinc the presumed dissociation constant for dimerization is approximately 1 μM, which is 100-fold lower than in the absence of Zn(II). These results support the notion that it is in fact a zinc-induced dimerization process that produces the FRET signal.

Stabilization of Obligate Heterodimers of CFP and YFP. In all the constructs presented above, the metal-ion sites were built symmetrically in both CFP and YFP to obtain as efficient a stabilization of the dimers as possible. In theory, each dimer will in this way be stabilized by two symmetric metal-ion sites. However, the tradeoff is that only half of the complexes will in fact be the desired heterodimers between CFP and YFP. The other half will be metal-ion site stabilized homodimers, which will be unable to produce FRET (Figure 8). To stabilize preferentially the FRET productive heterodimeric form between a CFP and a YFP molecule and not the unproductive homodimeric forms, we constructed a pair of molecules in which only half of a metal-ion site was introduced in each spectral variant of GFP, i.e., [S208C]-CFP and [Y39H]-YFP (Figure 8). The potency of Zn(II), EC_{50} = 1.0 mM, in inducing FRET was in this mixture slightly lower than in the mixture of CFP and YFP having the potential of forming two of these sites, [Y39H,-S208C]-CFP and [Y39H,S208C]-YFP, EC_{50} = 0.7 mM (Figure 8). Importantly, despite the fact that each dimer could only be stabilized by one metal-ion site, the maximally achievable FRET signal was increased from 4.6 to 8.2 (Figure 8).

DISCUSSION

Because FRET is highly dependent on the distance between the donor and the acceptor and due to the unfavorable location of the fluorophore deep inside the GFP molecule, "proximity" is not always enough to obtain FRET between spectral variants of GFP. It has been argued that FRET would occur with about 90% efficiency in a heterodimer corresponding to the homodimer found in the X-ray structure of GFP but formed between the cyan and the yellow spectral variant of GFP (*4*). In the present study, various attempts were made to stabilize such dimers by constructing zinc-ion sites around the dimerization interface of CFP and YFP.

Increased FRET Efficiency in the Metal-Ion Site Engineered GFP Variants. The basic metal-ion site of the present study was constructed as a bidentate site with one potential metal-ion coordinating residue located on each monomer, i.e., Tyr^{39} to His on one and Ser^{208} to Cys on the other. In the constructs where this site was made symmetrically in the two monomers to try to obtain as efficient a dimerization as possible by having each dimer stabilized by two metal-ion sites, Zn(II) dose-dependently induced FRET with a maximal signal of 4.8 (i.e., the I_{530}/I_{475} ratio). This indicates that efficient zinc-ion stabilized dimerization is in fact obtained with the metal-ion site engineered constructs. However, in this CFP/YFP construct just as in the wild-type proteins only half of the dimers will be of the desired FRET-producing heterodimeric form as the metal-ion will stabilize also the homodimers equally well (sketch in Figure 8). As expected, or rather hoped for, a higher FRET signal of 8.2 was obtained in the construct where only a single "half" metal-ion site was built into each of the spectral variants of GFP. Here Zn(II) would consequently only be able to stabilize FRET-productive heterodimers, albeit with only a single metal-ion site per dimer (sketch in Figure 8). This shows that recruitment of a larger fraction of the population of potential FRET signaling molecules by biasing for formation of heterodimers is one way of obtaining a more efficient FRET signaling. In biological systems where protein−protein interactions are studied, this would obviously to a large degree be taken care of by the fact that one spectral variant will be fused to one molecule and another spectral variant to the other protein. However, in cases where homodimerization of, for example, membrane receptors, would be studied, it could be an advantage to use altered spectral variants of GFP, which preferentially will form heterodimers.

Two attempts were made to construct tridentate zinc-binding sites in the CFP/YFP dimerization interface. The maximal zinc-induced FRET signals obtained with these constructs was comparable or slightly superior to the signal observed for bidentate engineered, obligate heterodimer forming pair (Figures 5 and 8). We would expect the mixtures of CFP and YFP with two tridentate sites to be able to form both zinc-stabilized hetero- and homodimers equally well since the sites were constructed symmetrically in the two molecules (see Figure 5). It cannot, however, be excluded that the [S208C,F223H,T225H]-CFP and [S208C,-F223H,T225C]-YFP FRET pairs favor formation of heterodimers and that more than 50% heterodimers are formed with these molecules. This could explain the observed difference in FRET signal between the two FRET pairs with two potential tridentate sites. Since no increase in metal-ion affinity was observed (see below) with the triple mutants as compared to the double mutants, it is possible that no actual tridentate coordination of the metal-ion in fact occurs in these constructs, but that the introduction of the extra metal-ion coordinating residues merely introduces a couple of extra possibilities for forming bidentate sites and possibly for keeping a higher local concentration of the metal-ion.

An alternative explanation for the increased FRET signaling induced by Zn(II) in the mutant proteins could, besides

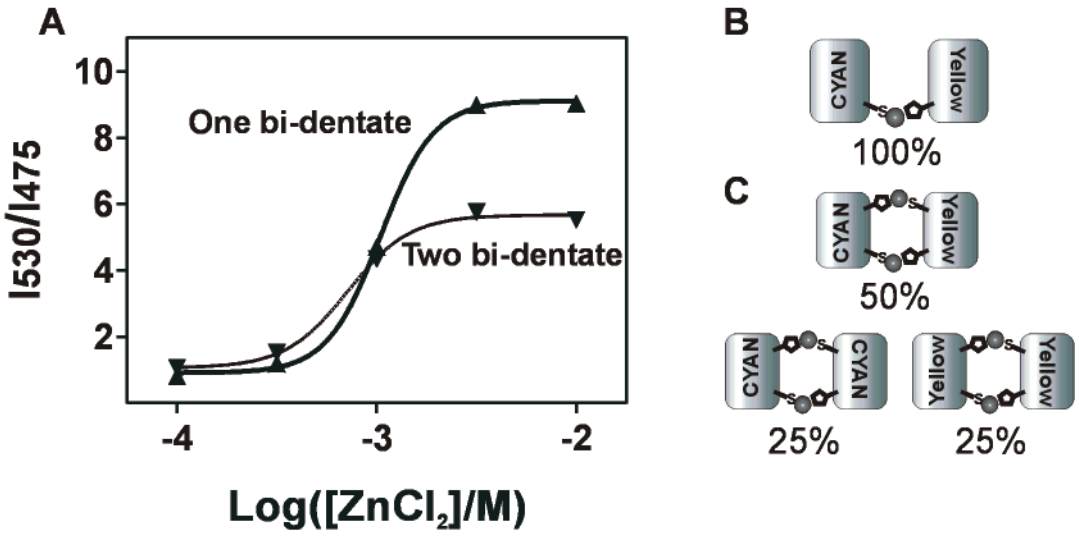

FIGURE 8: FRET in metal-ion site engineered spectral variants of GFP designed to form obligate heterodimers. Panel A: FRET signal, i.e., I_{530}/I_{475} ratio, in the [S208C]-CFP/[Y39H]-YFP pair (▲), designed to favor heterodimerization as compared to the [Y39H,S208C]-CFP/[Y39H,S208C]-YFP pair (▼) expressing two sites and therefore allowing for both homo- and heterodimerization. The experiments were made as triplicates; error bars indicate SEM. Panel B: schematic drawing of the [S208C]-CFP/[Y39H]-YFP pair stabilized by one Zn-(II)-ion (sphere). Panel C: schematic drawing of the theoretic combinations of [Y39H,S208C]-CFP and [Y39H,S208C]-YFP in the presence of Zn(II). Both hetero- and homodimerization are allowed, giving rise to 50% heterodimers and 50% homodimers.

the intended stabilization of dimers, be a Zn(II)-induced altered orientation of the two spectral variants in relation to each other in the heterodimers. The reason is that due to the fixed position of the chromophore within the GFP protein and the fact that the relative orientation between the two dipole moments of a FRET donor and an acceptor an altered angle between the two GFP variants could very well change the efficiency of the FRET signaling.

However, that the Zn(II) induced increase in FRET signaling most likely is caused by a simple stabilization of the dimers of the spectral variants of GFP was directly supported by the experiments showing a leftwards 100-fold shift in the concentration dependency of the FRET signal (Figure 6).

Zinc Affinity. Although an improvement of the FRET signal was achieved through the supposed stabilization of the optimal form of CFP and YFP by the engineered metal-ion sites, this was only observed at relatively high, 10^{-3} M, concentrations of $ZnCl_2$. When similar, bidentate metal-ion sites were engineered between the transmembrane helices of 7TM G-protein coupled receptors, the affinities for Zn-(II) were found to vary between 10^{-4} and 10^{-5} M (*17*−*20*). In these systems, tridentate sites having an affinity of 10^{-6} M have been constructed (*18*−*20*), whereas attempts to construct tridentate sites in the spectral variants of GFP only resulted in apparent zinc affinities of 10^{-3} M. Presumably, the relatively poor apparent affinity for Zn(II) in the metal-ion sites of the present study may be caused by the very high degree of rigidity in the solid β-barrel or β-can structure of GFP upon which the metal-ion coordinating residues are built. Conceivably, in the GFP variants, it is only structural alterations of the side chain as such that can be exploited to try to coordinate the metal-ion in this system. In contrast, in the 7TM receptors and in many other proteins previously used for metal-ion site engineering, a certain degree of adaptability or induced fit also of the backbone could be expected to "help" bring one metal-ion binding moiety into an optimal geometry in relation to the partnering, metal-ion binding residues. Nevertheless, it is likely that the present constructs cannot directly be used for studies of protein−protein interactions in cellular contexts since millimolar concentrations of Zn(II) in itself is not likely to be reached under physiological conditions.

Conclusion. The results of the present study demonstrate that the relatively weak FRET signal obtained at a given concentration of a mixture of CFP and YFP can be highly enhanced by stabilizing the formation of the heterodimer in which the two fluorophores are brought into as close as possible proximity and in a favorable relative orientation. The dimerization process between the spectral variants of GFP was in this study strengthened through metal-ion site engineering; however, many other forms of protein engineering could be exploited to obtain this. In could be envisioned that the dimerization interface could be altered in a way that would favor heterodimerization and at the same time would disfavor homodimerization; for example, a salt bridge could be introduced, which would stabilize a heterodimer and perhaps would cause a steric clash in the homodimer.

ACKNOWLEDGMENT

We thank Dr. Ulrik Gether for providing access to the spectrofluorometer.

REFERENCES

1. Misteli, T., and Spector, D. L. (1997) *Nat. Biotechnol. 15*, 961−964.
2. Pollok, B. A., and Heim, R. (1999) *Trends Cell Biol. 9*, 57−60.
3. Stryer, L. (1978) *Annu. Rev. Biochem. 47*, 819−846.
4. Tsien, R. Y. (1998) *Annu. Rev. Biochem. 67*, 509−544.
5. Day, R. N. (1998) *Mol. Endocrinol. 12*, 1410−1419.
6. Mahajanm, N. P., Linder, K., Berry, G., Gordon, G. W., Heim, R., and Herman, B. (1998) *Nat. Biotechnol. 16*, 547−552.
7. Xu, X., Gerad, A. L., Huang, B. C., Anderson, D.C., Payan, D. G., and Luo, Y. (1998) *Nucleic Acids Res. 26*, 2034−2035.

8. Miyawaki, A., Llopis, J., Heim, R., McCaffery, J. M., Adams, J. A., Ikura, M., and Tsien, R. Y. (1997) *Nature 388*, 882−887.
9. Nagai, Y., Miyazaki, M., Aoki, R., Zama, T., Inouye, S., Hirose, K., Iino, M., and Hagiwara, M. (2000) *Nat. Biotechnol. 18*, 313−316.
10. Suzuki, Y., Yasunaga, T., Ohkura, R., Wakabayashi, T., and Sutoh, K. (1998) *Nature 396*, 380−383.
11. Yang, F., Moss, L. G., and Philips, G. N., Jr. (1996) *Nat. Biotechnol. 14*, 1246−1251.
12. Ormö, M., Cubitt, A. B., Kallio, K., Gross, L. A., Tsien, R. Y., and Remington, S. J. (1996) *Science 273*, 1392−1395.
13. Youvan, D. C., Silva, C. M., Bylina, E. J., Coleman, W. J., Dilworth, M. R., and Yang, M. M. (1997) *Biotechnology 3*, 1−18.
14. Philips, G. N., Jr. (1997) *Curr. Opin. Struct. Biol. 7*, 821−827.
15. Horton, R. M., Hunt, H. D., Ho, S. N., Pullen, J. K., and Pease, L. R. (1989) *Gene 77*, 61−68.
16. Chakrabarti, P. (1990) *Protein Eng. 4*, 57−63.
17. Elling, C. E., and Schwartz, T. W. (1996) *EMBO J. 15*, 6213−6219.
18. Thirstrup, K., Elling, C. E., Hjorth, S. A., and Schwartz, T. W. (1996) *J. Biol. Chem. 271*, 7875−7878.
19. Lu, Z. L., and Hulme, E. C. (2000) *J. Biol. Chem. 275*, 5682−5686.
20. Elling, C. E., Nielsen, S. M., and Schwartz, T. W. (1995) *Nature 374*, 74−77.

BI001765M